Are two modes of thermohaline circulation stable?

By SYUKURO MANABE[1]* and RONALD J. STOUFFER[2], [1]*Institute for Global Change Research/FRSGC, Tokyo, Japan;* [2]*Geophysical Fluid Dynamics Laboratory/NOAA, Princeton University, Princeton, NJ 08542, USA*

ABSTRACT

The standard version of the coupled ocean–atmosphere model developed at the Geophysical Fluid Dynamics Laboratory (GFDL) of NOAA has at least two stable equilibria. One has a realistic and active thermohaline circulation (THC) with sinking regions in the northern North Atlantic Ocean. The other has a reverse THC with extremely weak upwelling in the North Atlantic and sinking in the Circumpolar Ocean of the Southern Hemisphere. Although the model has the seasonal variation of insolation, the structure of these two stable equilibria are very similar to those of a previous GFDL model without the seasonal variation. It is noted that the inactive mode of the reverse THC mentioned above is not a stable equilibrium for another version of the same coupled model which has a large coefficient of vertical subgrid scale diffusion. Although the reverse THC cell was produced in the Atlantic Ocean by a massive discharge of freshwater, it began to transform back to the original direct THC as soon as the freshwater discharge was terminated. It appears that there is a critical value of diffusivity, above which two stable equilibria do not exist. Based upon paleoceanographic evidence, we suggest that the stable state of the reverse THC mentioned above did not prevail during the cold periods of Younger Dryas event which occurred during the last deglacial period. Instead, it is likely that the THC weakened temporarily, but reintensified before it reached the state of the reverse THC with no deep water formation in the North Atlantic Ocean.

1. Introduction

Conducting the time integration of a general circulation model of the coupled ocean–atmosphere system with the annual mean insolation, Manabe and Stouffer (1988) obtained two stable equilibrium states: One state has realistic and active thermohaline circulation (THC), and the other has a weak, reverse THC without any deep water formation in the northern North Atlantic Ocean. It appears that these two states correspond to two stable equilibria of a simple box model of the THC identified by Stommel (1961).

As noted above, the model used by Manabe and Stouffer lacks the seasonal variation of insola-

tion. In winter, intense cooling of oceanic surface can facilitate the formation of deep water in the northern North Atlantic, significantly increasing the rate of deep water formation and destabilizing the reverse mode of the THC. Here, we demonstrate that, despite the inclusion of the seasonal variation of insolation, the coupled ocean–atmosphere model developed at Geophysical Fluid Dynamics Laboratory (GFDL) of NOAA does indeed possesses two stable equilibria which are very similar to what are obtained from a model with annually averaged insolation.

Recently, the existence of the stable state of weak, reverse THC is questioned by Schiller et al. (1997). Using a coupled model with seasonal variation of insolation developed at the Max-Planck Institute for Meteorology (MPI), they produced the reverse THC with no North Atlantic deep water formation

* Corresponding author.

through a massive discharge of freshwater at the surface of the northwest Atlantic Ocean. Upon termination of the freshwater discharge, however, the THC in the North Atlantic reintensified and regained its original intensity after a few hundred years. Based upon the results from this numerical experiment, they inferred that the state of the reverse THC with no North Atlantic deep water formation is not a stable state.

At GFDL, we also induced the state of the weak, reverse THC using a coupled ocean–atmosphere model with seasonal variation of insolation. In response to the prescription of very low surface salinity (i.e., 28 psu) in the northern North Atlantic over the period of 100 years, the state of the active THC, which was produced by the control integration, collapsed into the state of the reverse THC with extremely weak upwelling in the North Atlantic Ocean. Although the time integration of the coupled model was continued several thousand years after terminating the prescription of low surface salinity in the northern North Atlantic, the state of the THC remains inactive, in sharp contrast to the results obtained by Schiller et al. (1997).

We speculate that the different behavior of the MPI and GFDL coupled models mentioned above may be attributable to the difference in the magnitude of diapycnal diffusion. For the computation of advection terms, the oceanic component of the MPI coupled model (with 11 vertical finite difference levels and grid spacing of 5.6° longitude × 6° latitude) employs the first order, upstream finite difference technique which could yield large computational diffusion (see, for example, Wurtele, 1961 and Molenkamp, 1968). In such a diffusive model, the production of negative buoyancy resulting from the upward displacement of watermass over a given distance is relatively small, facilitating the reintensification of the THC in the numerical experiment conducted by Schiller et al. (1997). In the present study, we investigate how the stability and the structure of the two modes of the THC depend upon the magnitude of the vertical diffusion coefficient in a oceanic component of a coupled model. For this paper, we used two versions of the GFDL coupled model with the normal and large vertical diffusion coefficients. Based upon the results from this and other studies, the stability and existence of these two modes in the real ocean of past and present are discussed.

The next section describes the structure and time integration of the GFDL coupled ocean–atmosphere model with seasonal variation of insolation. The structure of the two stable equilibria of the THC obtained from the standard version of the GFDL coupled model is described briefly in Section 3. Section 4 contains the results from the freshwater experiment which was conducted using another version of the same coupled model with a much larger coefficient of the vertical subgrid–scale diffusion. Finally, the concluding section discusses the existence and stability of the state of the reverse THC with no deep water formation in the Atlantic Ocean.

2. Coupled model

2.1. Model structure

The coupled atmosphere–ocean–land surface model used in this study was developed for studying the climate response to increasing greenhouse gases, and is called the coupled model for simplicity. The structure and performance of the coupled model were described briefly by Stouffer et al. (1989) and in more detail by Manabe et al. (1991,1992), and Manabe and Stouffer (1994). The model consists of a general circulation model (GCM) of the global atmosphere coupled to a GCM of the oceans. Heat, water, and snow budgets at the continental surface are included. The coupled model has global geography consistent with its computational resolution, and seasonal (but not diurnal) variation of insolation.

In the atmospheric component of the coupled model, dynamic computations are performed using the so–called spectral element method (Orszag, 1970; Gordon and Stern, 1982), in which the distribution of a predicted variable is represented by a set of spherical harmonics (with 15 zonal waves and 15 associated Legendre functions) and is specified at grid points of 4.5° latitude and 7.5° longitude intervals. There are nine unevenly spaced levels in the vertical. The effects of clouds, water vapor, carbon dioxide, and ozone are included in the calculation of both solar and terrestrial radiation. Water vapor and precipitation are predicted by the model (Manabe et al., 1965), but a constant mixing ratio of carbon dioxide and a zonally uniform, seasonally varying vertical distribution of ozone are prescribed. Overcast cloud is assumed whenever relative

humidity exceeds a critical value. Otherwise, clear sky is predicted.

The ocean model of Bryan and Lewis (1979) has been modified as described by Manabe et al. (1991). The finite–difference mesh used for the time integration of the primitive equations of motion has a spacing between grid points of about 4.5° latitude and 3.7° longitude. It has 12 unevenly spaced levels in the vertical. In addition to the horizontal and vertical background subgrid-scale mixing and convective overturning, the coupled model has isopycnal mixing as described by Redi (1982) and Tziperman and Bryan (1993). For the specific choice of parameters in the formulation of subgrid scale mixing processes other than vertical diffusion, see Manabe et al. (1991). The coupled model predicts sea ice using a simple scheme that incorporates the thermodynamics and horizontal advection of sea ice by ocean currents (Bryan, 1969).

The present study employs two versions of the coupled model which are identical to each other with the exception of the magnitude of the vertical subgrid-scale diffusion coefficient. Fig. 1 illustrates
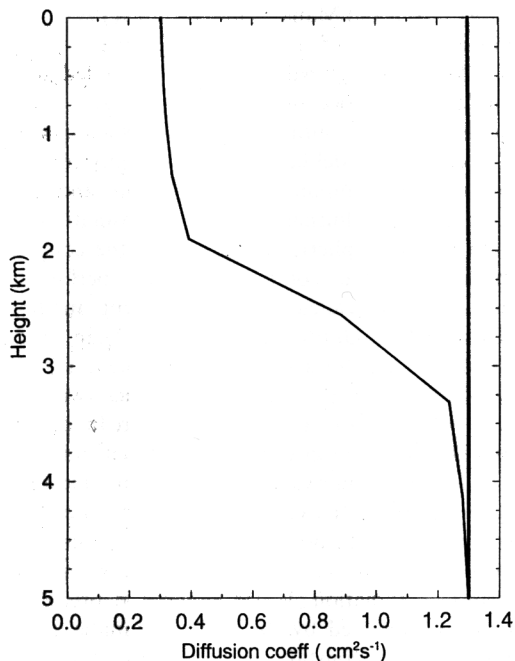

Fig. 1. Vertical distributions of the vertical subgrid-scale diffusion coefficient (cm^2 s^{-1}). Thin line: Standard version. Thick line: LVD version.

the two profiles of the vertical diffusion coefficient. The first profile (thin line) was originally proposed by Bryan and Lewis (1979) and has been incorporated in the standard version of the present coupled model. This profile was determined based upon the measurement of Gregg (1977) that vertical mixing is lowest within the thermocline and increases below the thermocline. On the other hand, the second profile (thick line) is incorporated into the LVD (large vertical diffusion) version of the coupled model in order to investigate the structure of the THC as influenced by a large vertical diffusion coefficient.

2.2. Initial condition and flux adjustment

The initial conditions for the time integration of the coupled model have seasonal and geographical distributions of observed sea surface temperature (SST), sea surface salinity (SSS), and sea ice with which both the atmospheric and oceanic model states are nearly in equilibrium (see Manabe et al. (1991) for the computational procedure which is used for obtaining the initial condition). When the time integration of the model starts from this initial condition, the model climate drifts toward its own equilibrium state, which differs from the initial condition. To reduce this drift, the fluxes of heat and water imposed at the oceanic surface (including sea ice-covered areas) of the coupled model are modified by amounts that vary geographically and seasonally but do not change from one year to the next [see Manabe et al. (1991) and Manabe and Stouffer (1994) for details]. Since the adjustments are determined prior to the time integration of the coupled model and are not correlated to the transient anomalies of SST and SSS, which can develop during the integration, they are unlikely to either systematically amplify or damp the anomalies. Owing to the flux adjustment technique described above, both SST and SSS of the coupled model fluctuates around a realistic values. One should also note, however, that this technique is quite different from the "restoring" that has been applied to SST and SSS during the time integration of an ocean-only model (e.g., Bryan and Cox, 1967), which strongly damps surface anomalies.

The initial condition is also computed for the high resolution version of the coupled model. Although the geographical distributions of initial

SST and SSS are very similar between the two versions, the deep water temperature obtained from the LVD version of the coupled model is warmer than that of the standard version by more than 1°C because of larger downward diffusion of heat. It turned out that the magnitude of water and heat flux adjustments, which are required for maintaining realistic surface conditions, differs slightly between the two versions of the coupled model.

3. Two stable equilibria

3.1. Time integration

Control integration. Starting from the initial condition described in section 2.2, the standard version of the coupled model with the flux adjustment was integrated over the period of 8000 years. Owing to the application of the flux adjustment, the trend of the globally averaged, surface air temperature is only −0.023°C/century during the first 1000 years. The trend becomes much smaller during the remainder of the integration. On the other hand, the trend of global mean temperature in the deeper ocean at the depth of 3 km is −0.07°C/century during the first 1000 years. However, this trend also becomes very small toward the end of the 8000-year integration (Fig. 2), indicating that the coupled model is very
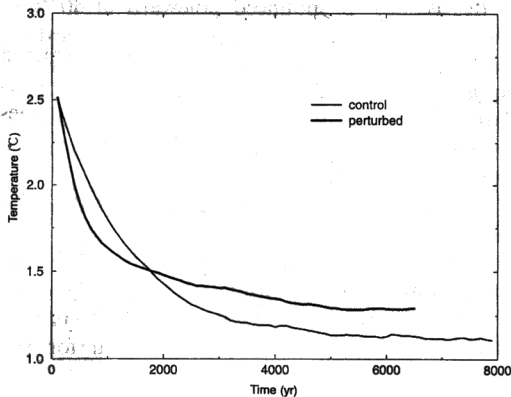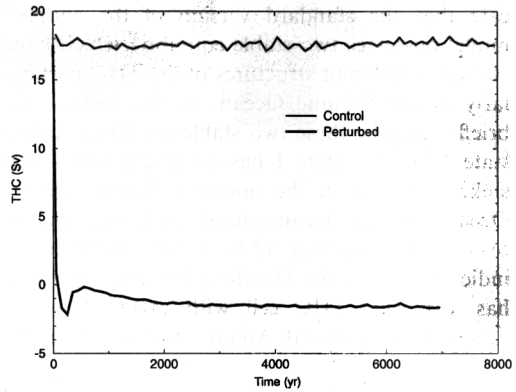
Fig. 3. Time series of 100-year mean intensity of the THC (in units of Sverdrups, i.e., 10^6 m^3 s^{-1}) in the North Atlantic Ocean. Thin line: control integration. Thick line: perturbed integration. The intensity of the THC is defined as the maximum value of the streamfunction of meridional overturning circulation.

close to the state of thermal equilibrium. In the North Atlantic Ocean of the coupled model, the THC remains active and its intensity remains around 17 Sv throughout the course of the 8000-year integration (Fig. 3).

Perturbed integration. The control integration described above is perturbed by restoring the surface salinity to a very low value of 28 psu in the zonal belt from 50°N to 70°N latitude in the North Atlantic Ocean over a 100 year period, inducing the state of the reverse THC with no ventilation of subsurface water in the North Atlantic Ocean. Despite the cessation of the surface salinity restoration, the THC remains inactive during the remainder of the 7000-year integration (Fig. 3). The globally averaged, deep water temperature decreases slowly and levels off eventually with no sign of warming (Fig. 2). The results indicate that the coupled model is very close to the state of equilibrium towards the end of the integration. Towards the end of the integration, the temperature of bottom water is maintained as the balance between the heating due to vertical diapycnal diffusion and the cooling due to the Antarctic bottom water formation.

Fig. 2. Time series of globally averaged, 100-year mean oceanic temperature (°C) at the depth of 3 km obtained from the standard version of the coupled model. Thin line: control integration. Thick line: perturbed integration.

3.2. Structure

The results from the control and perturbed integrations described in Subsection 3.1, indi-

cate that the standard version of the coupled model possesses two stable equilibria which have two quite different structures of the THC particularly in the Atlantic Ocean. In this section, we briefly describe these two stable equilibria, called state I and II. State I has an active THC with sinking regions in the northern North Atlantic Ocean. The time mean rate of the North Atlantic overturning is about 17 Sv (1 Sv = 10^6 m³/s) as indicated in Fig. 4a. On the other hand, state II has a reverse THC cell with extremely weak upwelling in the North Atlantic and sinking in the
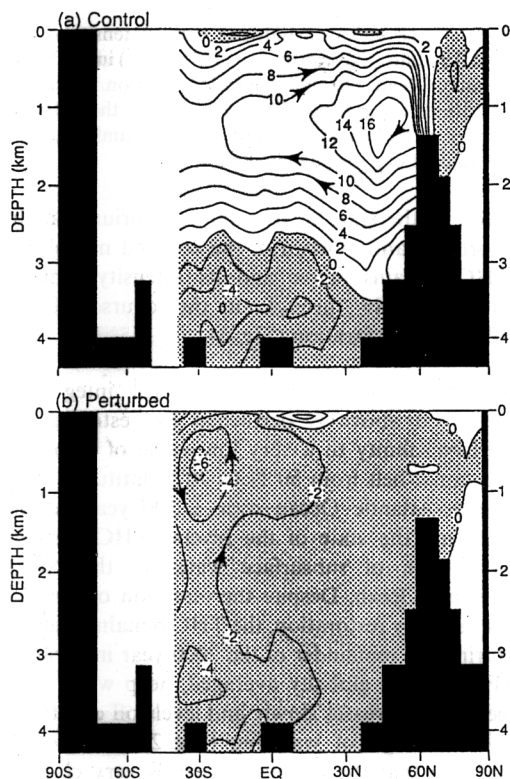

Fig. 4. The latitude–depth distributions of the streamfunction of the thermohaline circulation (THC) in the Atlantic Ocean obtained from the standard version of the coupled ocean–atmosphere model. Upper and lower panels (a) and (b) represent the streamfunctions of meridional circulation averaged over the years 5901–6000 of the control and perturbed integrations, respectively. Units are in Sverdrups (i.e., 10^6 m³/s). The silhouette of the bottom topography in the Atlantic Ocean of the coupled model, as seen in a zonal direction, is covered by black, resulting in the penetration of streamfunction contours into the bottom topography.
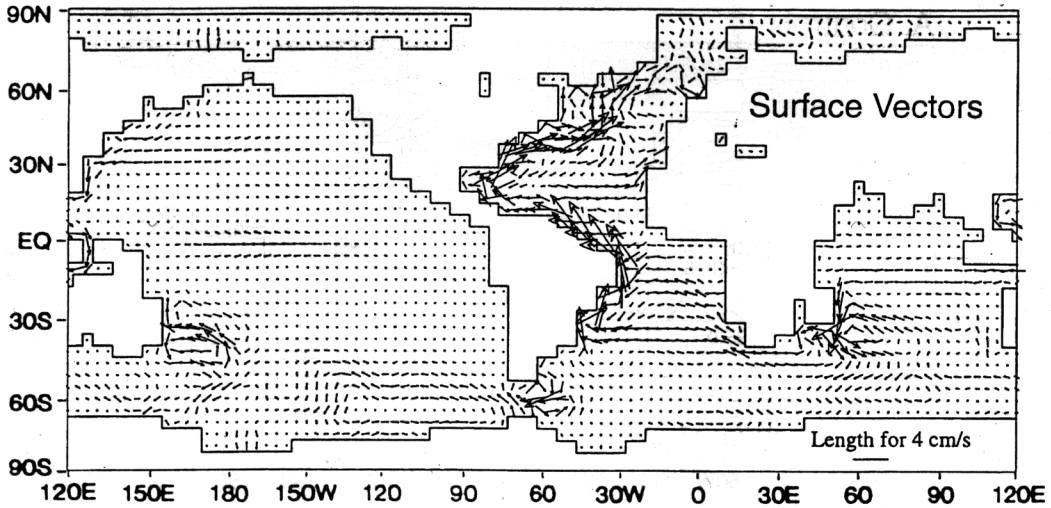
Circumpolar Ocean of the Southern Hemisphere (Fig. 4b). It has no ventilation of subsurface water in the North Atlantic Ocean.

In order to examine the surface currents associated with the Atlantic THC, the geographical distribution of the difference in surface currents between the state I and II is illustrated in Fig. 5 by vectors. As this figure indicates, the surface currents associated with the THC in the Atlantic Ocean pass through the Indonesian Passage, move westward in the tropical part of the Indian Ocean, and move northwestward in the South Atlantic, eventually reaching the northern North Atlantic or Nordic Seas where the sinking of water and deep water formation take place. The distribution of surface currents closely resembles the surface manifestation of the "conveyor belt" determined, for example, by Gordon (1986).

Fig. 6 illustrates the geographical distributions of surface salinity of the equilibrium states I and II and the difference between them. In the North Atlantic Ocean, surface salinity of state I is larger than that of state II. The difference is particularly large around the Denmark Strait by as much as 3 psu (Fig. 6c). The northward advection of saline surface water from the subtropics by the THC is responsible for maintaining the relatively high surface salinity in state I compared with state II. The difference in the rest of the world is negative but is very small.

The sea surface temperature is significantly warmer in state I than state II in the North Atlantic (Fig. 7). The difference between the two states is most pronounced poleward of 40°N in the Atlantic Ocean. As noted with regard to surface salinity, the northward advection of warm surface water by the THC from the tropics to high latitudes helps maintain the relatively high surface salinity in the North Atlantic in state I, whereas such advection is missing in state II.

The two stable equilibria of the coupled model described above are very similar to those of a previous GFDL coupled model without the seasonal variation of insolation (Manabe and Stouffer, 1988). The present result suggests that the seasonal variation is not required for the existence of two stable equilibria.

4. Large diapycnal diffusion

As speculated in the introduction, state II with the reverse THC and sinking in the Circumpolar

Fig. 5. Vector difference in surface currents between the control and perturbed integrations (i.e., the states I and II) of the standard version of the coupled ocean–atmosphere model. The difference vectors represent the time means over years 5901–6000 of both integrations.

Ocean of the Southern Hemisphere could be unstable in a coupled model with larger diapycnal diffusion. This is because the vertical movement of water across isopycnal surfaces is easier in an oceanic general circulation model using a larger vertical subgrid-scale diffusion coefficient. In such a model, a given watermass tends to lose its identity and negative buoyancy as it rises in a stable environment, facilitating the reintensification of the THC. Furthermore, a model with larger vertical diffusion has smaller static stability, producing smaller negative buoyancy for a given upward displacement of watermass. Thus, the mode of reverse THC could become unstable and transform into the mode of active THC through the reintensification of the upwelling in the Atlantic Ocean.

In order to confirm this speculation, we constructed another version (i.e., the LVD version) of the coupled model, which has a large coefficient of vertical subgrid-scale diffusion in the thermocline as described in Subsection 2.1 (Fig. 1). Both the control and perturbed integrations were conducted using the LVD version of the coupled model.

Starting from an initial condition, which was constructed in the same way as we did for the time integration of the standard version (Subsection 2.2), the control integration was performed over a period of 4000 years. Throughout the integration, the global mean surface air temperature has almost no systematic trend and the THC remains active in the North Atlantic Ocean. The intensity of the THC, which remains around 29 Sv (Fig. 8), is much larger than 17 Sv obtained from the control integration of the standard coupled model (compare Fig. 4a and Fig. 9a which illustrate the streamfunction of the Atlantic THC obtained from the standard and LVD versions of the coupled model, respectively). The results indicate that the model with higher vertical diapycnal diffusion coefficient has a stronger THC. Bryan (1987) noted a qualitatively similar dependence of the THC intensity upon the magnitude of the vertical diffusion coefficient. Because of the compensation between the heating of the thermocline water due to vertical diffusion and its cooling due to the advection of potential temperature by upward motion, it is possible to maintain the stronger THC in the more diffusive ocean.

The perturbed integration of the LVD version of the coupled model started from year 500 of the control integration. During the first 100 years of the experiment, freshwater is discharged uniformly into the 50°N to 70°N belt of the North Atlantic Ocean at the rate of 1 Sv (i.e., $10^6 \, \text{m}^3/\text{s}$). The
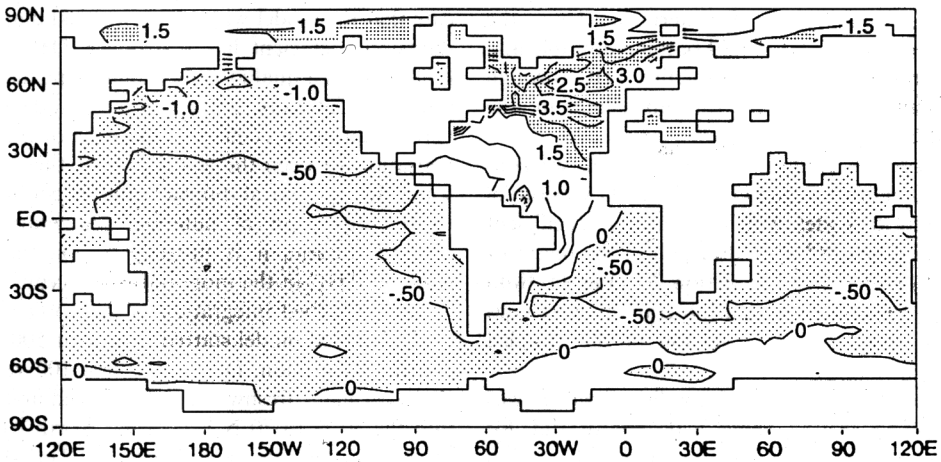
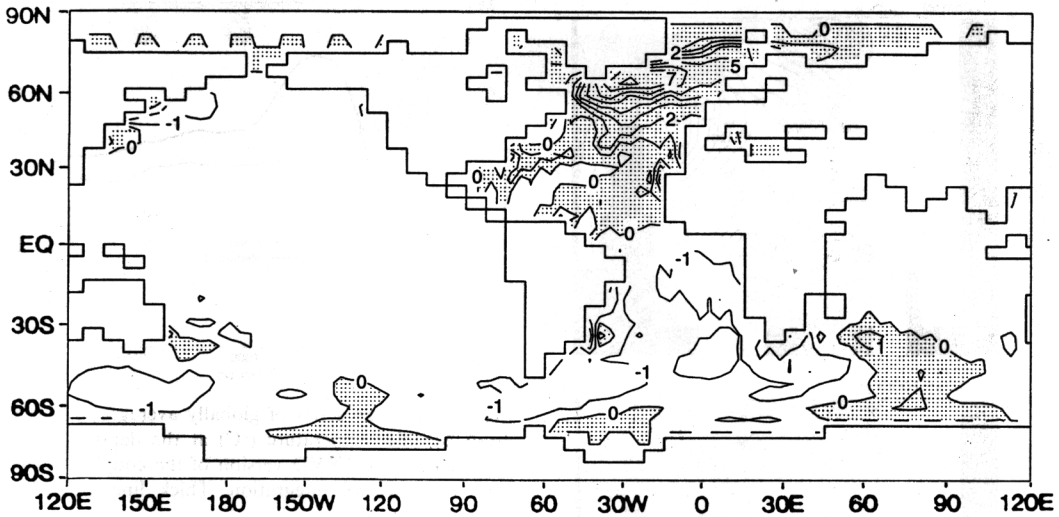A. Control
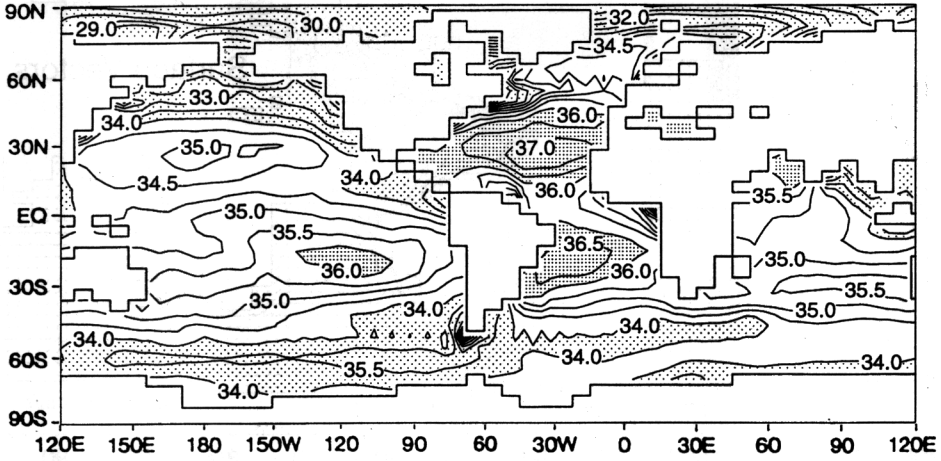
B. Perturbed
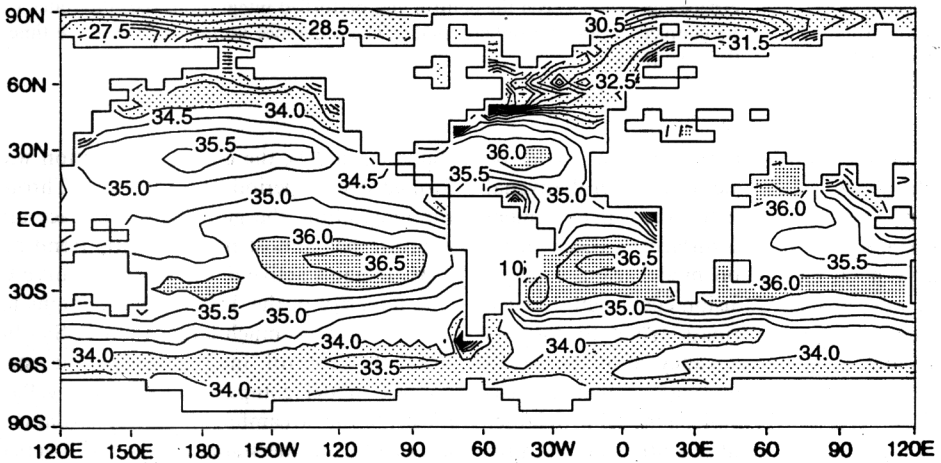
C. Difference

Fig. 7. Geographical distribution of sea surface temperature difference (°C) between the control and perturbed integrations (i.e., states I and II) of the standard version of the coupled ocean–atmosphere model. The sea surface temperatures represent time averages over years 5901–6000 of both integrations.
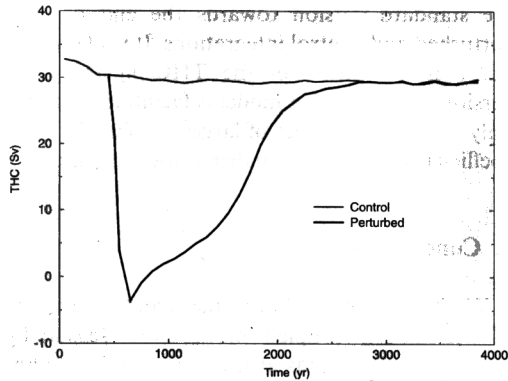

Fig. 8. The time series of 100-year mean intensity of thermohaline circulation in the North Atlantic Ocean obtained from the LVD version of the coupled ocean–atmosphere model. Thin line: control integration. Thick line: perturbed integration. Units are in Sverdrups (i.e., 10^6 m^3/s).

massive input of freshwater described here has very similar effect on the THC as the restoration of surface salinity towards a very low value, which was employed earlier (i.e., Subsection 3.1) in order

to induce the inactive mode of the reverse THC in the standard version of the coupled model. As indicated in Fig. 8, the THC in the North Atlantic Ocean weakens rapidly and reverses direction towards the end of the 100-year period. The streamfunction of the reverse THC at the end of this period is illustrated in Fig. 9b, which indicates weak upwelling in the North Atlantic and sinking in the Circumpolar Ocean of the Southern Hemisphere. Upon termination of the freshwater discharge, however, the THC in the Atlantic Ocean reverses direction again and regains its original intensity (Fig. 9c), in sharp contrast to the behavior of the standard version of the model. After undergoing large fluctuations, the global mean temperature of the deep water also approaches asymptotically the value reached by the control integration (Fig.10). These results indicate that the state of the reverse THC is not a stable equilibrium for the LVD version of the coupled model.

In both control and perturbed integrations of the LVD version of the coupled model, the global mean oceanic temperature at the depth of ~3 km

Fig. 6. (a) and (b) illustrate the geographical distributions of sea surface salinity (psu) averaged over years 5901–6000 of the control and perturbed integrations (i.e., the states I and II), respectively, of the standard version of the coupled ocean–atmosphere model. (c) illustrates the difference between (a) and (b).

Fig. 10. The time series of globally averaged, 100-year mean oceanic temperature (°C) at the depth of 3 km obtained from the LVD version of the coupled model. Thin line: control integration. Thick line: perturbed integration.

the static stability in the deep layer of the LDV version of the coupled model is less than those of the standard version towards the end of both perturbed and control integrations. It is likely that the reintensification of the THC in the LVD version of the coupled model is facilitated due not only to the direct effect of larger vertical diffusion coefficient but also to smaller static stability.

5. Conclusions

We have confirmed that the standard version of the GFDL coupled model with seasonally varying insolation has at least two stable equilibrium states. One state has a realistic and active THC with sinking in the northern North Atlantic Ocean. The other has a reverse THC with sinking in the Circumpolar Ocean of the Southern Hemisphere and no ventilation of subsurface water in the North Atlantic Ocean.

However, the reverse THC is not a stable equilibrium for another (LVD) version of the coupled model with a large vertical subgrid-scale diffusion coefficient. Although a reverse THC was induced in the Atlantic Ocean by a massive discharge of freshwater, it began to transform back to the active, direct THC as soon as the freshwater discharge was terminated. The results from the two versions of the coupled model indicate that there is a critical value of diffusivity above which
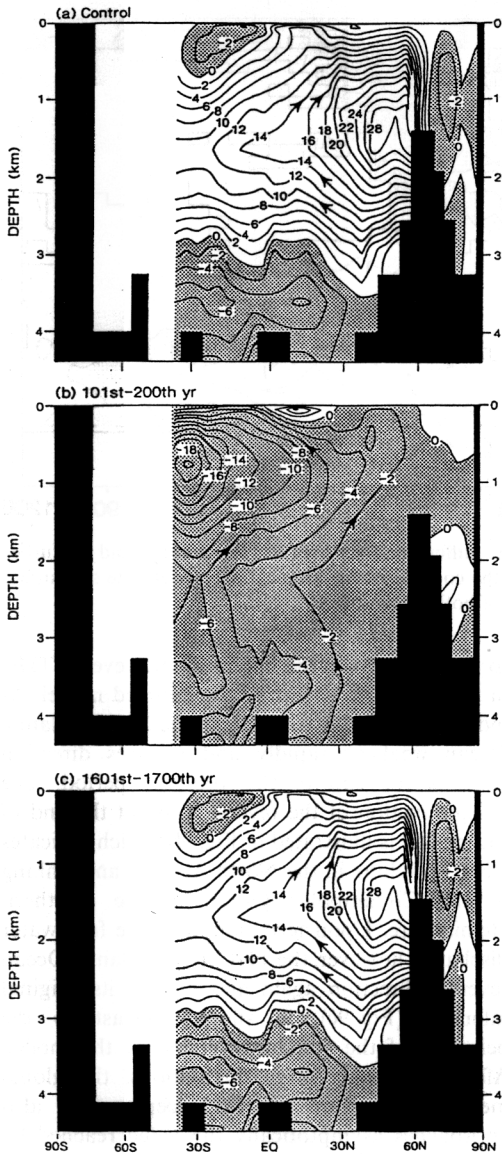
Fig. 9. The latitude–depth distributions of the stream-function of the thermohaline circulation (THC) in the Atlantic Ocean obtained from the LVD version of the coupled ocean–atmosphere model. Streamfunction is averaged over (a) years 2101–2200 of the control integration, and (b) years 101–200 and (c) years 1601–1700 of the perturbed integration.

approaches asymptotically 2.6°C, which is larger than 1.2°C reached in the integrations of the standard version of the coupled model. This implies that, because of large vertical diffusion,

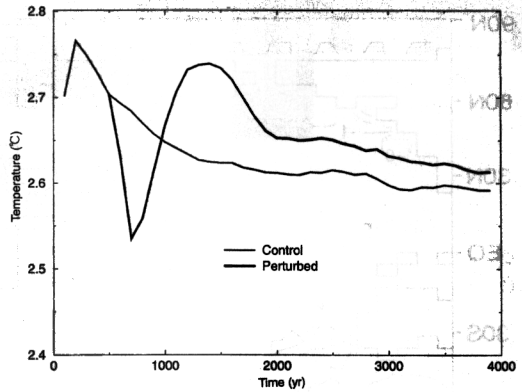two stable equilibria do not exist. In order to know whether the two stable equilibria exist in the real oceans or not, it is therefore necessary to determine the magnitude of vertical diapycnal diffusion in the oceans. Measurement of the invasion of anthropogenic tracers, such as bomb tritium and ^{3}He, have indicated that the coefficient of vertical diapycnal mixing in the ocean thermocline of the subtropical North Atlantic is less than 0.1 cm^2 s^{-1} (Jenkins, 1980) or about 0.2 cm^2 s^{-1} (Rooth and Östlund, 1972). The results from a recent field experiment, which injected an artificial tracer into the Atlantic Ocean, indicate that the most likely value of the coefficient of the vertical diapycnal diffusion in the ocean thermocline lies in the range between 0.1 and 0.2 cm^2/s (Ledwell et al., 1994). The vertical diffusion coefficient in the standard version of the coupled model is larger than these values. Therefore, it is likely that the real ocean has the stable mode of the reverse THC in addition to that of the direct THC.

Rahmstorf (1995) investigated the response of the THC to the input of freshwater using a global ocean circulation model coupled to a simplified model of the atmosphere. In response to very slowly increasing removal of freshwater (or addition of salt), for example, the inactive mode of the reverse THC becomes unstable and transformed into the active mode of the direct THC. Here, similar transformation occurred in the LVD version of the coupled model in response to the termination of freshwater supply. It appears that the increase of the vertical diffusion coefficient in the coupled model ocean make it possible to induce the transition from the inactive to active modes of the THC at larger meridional gradient of surface salinity.

The behavior of the LVD version of the coupled model described above resembles the response of the MPI coupled model to the massive discharge of freshwater (Schiller et al., 1997). As hypothesized in the introduction, the resemblance of behavior between the MPI model and the LVD version of our coupled model may be attributable to the large vertical diapycnal diffusion which is common to both models. It has been noted already that the MPI model employs the first order, upstream difference technique which yields large, implicit computational diffusion. On the other hand, the LVD version of our coupled model

employs an explicit, large vertical subgrid-scale diffusion coefficient.

The stable mode of the active THC obtained from the LVD version of the coupled model is more intense than that of the MPI model. As discussed in Section 4, the larger the vertical diffusion is, the stronger is the intensity of the THC. Accordingly, it is likely that the magnitude of the effective vertical diffusion of the MPI model is somewhere between the standard and LVD version of the coupled model.

Using coupled models in which a so-called energy balance model of the atmosphere is combined with an oceanic circulation model, Fanning and Weaver (1997) and Mikolajewicz (1996) obtained the mode of the reverse THC by discharging large amounts of freshwater in the North Atlantic Ocean. After termination of the freshwater discharge, the reverse THC in their models remains stable, in agreement with the behavior of our coupled model. When the effect of the "wind stress feedback" (Marotzke, 1989) was incorporated into their model, however, the mode of the normal, direct THC began to intensify very slowly and regained the original intensity over a millennium time scale, which is much longer than the restoration time of ~100 years obtained by Schiller et al. (1997). The behavior of their models described here, however, differs from the standard version of the GFDL coupled model, in which the mode of the reverse THC remains stable over very long time despite the termination of the freshwater discharge. It is likely that this difference results partly from the difference in vertical subgrid scale diffusion coefficient between the GFDL and other two models. For example, the value of vertical diffusion coefficient in the oceanic component of the GFDL coupled model shifts from 0.3 to 1.3 cm^2/s^{-1} at 2.5-km depth, i.e., well below the thermocline. On the other hand, the shifts between the two values occur around the depth of 1 km in the Fanning–Weaver model. Larger coefficient of vertical subgrid scale diffusion in the Fanning–Weaver model may be responsible for the difference in the behavior between the two models.

The oceanic component of the coupled model used by Mikolajewicz is similar to that used by Schiller et al. However, he modified the original code (Maier-Reimer et al., 1993) to include the explicit vertical diffusion of temperature and salinity. On the other hand, he increased the number

of vertical finite difference levels from 11 to 22, thereby reducing the computational diffusion which results from the first order, upstream differencing. Although it is difficult to determine the magnitude of effective oceanic diapycnal diffusion, one can speculate that the magnitude lies somewhere between the GFDL and original MPI models, yielding the results which was described by Mikolajewicz.

The different behavior between the GFDL and other two models may also be attributable to the different patterns and magnitudes of surface wind stress in the models. Specifically, the pattern of positive sea level pressure anomaly in our model is confined more towards Greenland, making it harder to reintensify the THC. Obviously, a more careful evaluation of the models is needed for a convincing determination of the basic cause of the difference. However, since the mode of the reverse THC is only marginally unstable in the models of Fanning–Weaver and Mikolajewicz, the use of smaller vertical diffusion coefficient could have stabilized the mode of the reverse THC in their models.

In order to confirm convincingly the existence of the inactive mode of the reverse THC, it is necessary to determine more accurately the magnitudes of diapycnal as well as isopycnal eddy diffusion in the ocean. In addition, it is highly desirable to repeat the experiments conducted here using a coupled model with much higher computational resolution which permit better representation of the THC and its interaction with the bottom topography.

Earlier, Manabe and Stouffer (1988) speculated that the inactive mode of the reverse THC prevailed in the North Atlantic Ocean during the cold period of Younger Dryas. However, paleoceanographic evidence does not necessarily support this speculation. Although the deep-sea cores from the North Atlantic Ocean indicate markedly reduced deep water formation (i.e., Boyle and Keigwin, 1987; Keigwin and Lehman, 1994), the

distribution of benthic $\delta^{13}C$ determined by Sarnthein et al. (1994) suggests that an upper deep-water production of significant magnitude did occur during the Younger Dryas. It appears that the state of the Younger Dryas in the Atlantic Ocean may be significantly different from the stable state of the reverse THC with no ventilation of subsurface water in the North Atlantic Ocean.

When the standard version of the coupled model produces the stable state of the reverse THC, it remains in that state. However, it appears that in the actual North Atlantic Ocean, the THC recovered its intensity very rapidly at the end of the cold Younger Dryas period inducing the abrupt warming. This is another important reason why we believe that, during the cold Younger-Dryas period, the stable mode of the reverse THC did not prevail in the North Atlantic Ocean.

Recently, Manabe and Stouffer (1995, 1997) conducted a series of numerical experiments exploring the response of the standard version of the coupled model to various types of freshwater discharge. They found that, if the freshwater discharge was terminated before the coupled model reaches the stable state of the reverse THC, the THC could reintensify upon termination of the discharge. Their experiment also indicates that, upon abrupt initiation and termination of the freshwater discharge, large oscillations of the THC with multidecadal time scale were generated, inducing large rise and fall of sea surface temperature in a few decades. Based upon the results of the numerical experiments described above, they suggested that the state of temporarily weakened THC (rather than the stable state of the reverse THC) be realized during the Younger Dryas. This suggestion appears to be consistent with the paleoceanographic evidence as noted above. However, further analysis of fast-accumulating cores in both East and West Atlantic is needed in order to confirm reliably the existence (or absence) of North Atlantic deep water formation during the Younger Dryas.

REFERENCES

Boyle, E. A. and Keigwin, L. D. 1987. North Atlantic thermohaline circulation during the past 20,000 years linked to high-latitude surface temperature. *Nature* **330**, 35–40.

Bryan, F. 1987. Parameter sensitivity of primitive equation ocean general circulation model. *J. Phys. Oceanogr.* **17**, 970–985.

Bryan, K. 1969. Climate and the ocean circulation (II). The ocean model. *Mon. Wea. Rev.* **97**, 806–827.

Bryan, K. and Cox, M. 1967. A numerical integration of the oceanic general circulation model. *Tellus* **19**, 54–80.

Bryan, K. and Lewis, L. 1979. A water mass model of the world ocean. *J. Geophys. Res.* **84**(C5), 2503–2517.

Fanning, A. F and Weaver, A. J. 1997. Temporal-geo-graphical meltwater influences on the North Atlantic conveyor: Implication for the Younger Dryas. *Paleoceanography* **12**, 307–320.

Gordon, A. L. 1986. Interocean exchange of thermohaline water. *J. Geophys. Res.* **91**(C4), 5037–5046.

Gordon, C. T. and Stern, W. 1982. A description of the GFDL global spectral model. *Mon. Wea. Rev.* **110**, 625–644.

Gregg, M. C. 1977. Variation in the intensity of small scale mixing in the main thermocline. *J. Phys. Oceanogr.* **7**, 436–454.

Jenkins, W. J. 1980. Tritium and ³He in the Sargasso Sea. *J. Marine Research* **38**, 533–569.

Keigwin, L. D. and Lehman, S. J. 1994. Deep circulation linked to Heinrich event 1 and Younger Dryas in a mid depth North Atlantic core. *Paleoceanography* **9**, 185–194.

Ledwell, J. R., Watson, A. J. and Law, C. S. 1994. Evidence for slow mixing across the pycnocline from an open-ocean tracer-release experiment. *Nature* **364**, 701–703.

Maier-Reimer, E., Mikolajewicz, U. and Hasselmann, K. H. 1993. Mean circulation of the LSG OGCM and its sensitivity to the thermohaline surface forcing. *J. Phys. Oceanogr.* **23**, 731–757.

Manabe, S. and Stouffer, R. J. 1997. Coupled ocean-atmosphere model response to freshwater input: Comparison to Younger Dryas event. *Paleoceanography* **12**, 321–336.

Manabe, S. and Stouffer, R. J. 1995. Simulation of abrupt climate change induced by freshwater input to the North Atlantic Ocean. *Nature* **378**, 165–167.

Manabe, S. and Stouffer, R. J. 1994. Multiple-century response of a coupled ocean-atmosphere model to an increase of atmospheric carbon dioxide. *J. Climate* **7**, 5–23.

Manabe, S. and Stouffer, R. J. 1988. Two stable equilibria of a coupled ocean-atmosphere model. *J. Climate* **1**, 841–866.

Manabe, S., Smagorinsky, J. and Strickler, R. F. 1965. Simulated climatology of general circulation model with a hydrologic cycle. *Mon. Wea. Rev.* **93**, 769–798.

Manabe, S., Spelman, M. J. and Stouffer, R. J. 1992. Transient response of a coupled ocean-atmosphere model to gradual change of atmospheric CO_2 (II). Seasonal response. *J. Climate* **5**, 105–126.

Manabe, S., Stouffer, R. J., Spelman, M. J. and Bryan, K. 1991. Transient response of a coupled ocean-atmosphere model to gradual change of atmospheric CO_2 (I). Annual mean response. *J. Climate* **4**, 785–818.

Marotzke, J. 1989. *Instabilities and multiple steady states of the thermohaline circulation in oceanic circulation models: combining data and dynamics.* NATO ASI Series 284, edited by D. L. T. Anderson and J. Willebrand, Kluwer Acad., Norwell, MA, pp. 501–511.

Mikolajewicz, U. 1996. *A meltwater induced collapse of the "conveyor belt" thermohaline circulation and its influence on the oceanic distribution of $\delta^{14}C$ and $\delta^{18}O$.* Max-Plank-Institut für Meteorologie, Rep. **189**, 25 pp.

Molenkamp, C. R. 1968. Accuracy of finite-difference methods applied to the advection equation. *J. Appl. Meteor.* **7**, 160–167.

Orszag, S. A. 1970. Transform method for calculating vector-coupled sums: Application to the spectral form of the vorticity equation. *J. Atmos. Sci.* **27**, 890–895.

Rahmstorf, S. 1995. Bifurcations of the Atlantic thermohaline circulation in response to change in the hydrologic cycle. *Nature* **378**, 145–149.

Redi, M. H. 1982. Oceanic isopycnal mixing by coordinate rotation. *J. Phys. Oceanogr.* **12**, 1154–1158.

Rooth, C. G. and Östlund, H. G. 1972. Penetration of tritium into the Atlantic thermocline. *Deep-Sea Research* **19**, 481–492.

Sarnthein, M., Winn, K., Jung, S. A., Duplessy, J.-C., Labeyrie, L., Erkenkeuser, H. and Gaussen, G. 1994. Changes in east Atlantic deep water circulation over the past 30,000 years: Eight times slice reconstructions. *Paleoceanography* **9**, 209–267.

Schiller, A., Mikolajewicz, U. and Voss, R. 1997. The stability of the North Atlantic thermohaline circulation in a coupled ocean-atmosphere general circulation model. *Climate Dynamics* **13**, 325–347.

Stommel, H. M. 1961. Thermohaline convection with two stable regimes of flow. *Tellus* **13**, 224–230.

Stouffer, R. J., Manabe, S., Spelman, M. J. and Bryan, K. 1989. Interhemispheric asymmetry in climate response to a gradual increase of atmospheric CO_2. *Nature* **342**, 660–662.

Tziperman, E. and Bryan, K. 1993. Estimating global air-sea fluxes from surface properties and from climatological flux data using an oceanic general circulation model. *J. Geophys. Res.* **98**(C12), 22,629–22,644.

Wurtele, M. G. 1961. On the problem of truncation error, *Tellus* **13**, 379–391.